Atmospheric Environment 291 (2022) 119406

Contents lists available at ScienceDirect

Atmospheric Environment

journal homepage: www.elsevier.com/locate/atmosenv

Field evidence for enhanced generation of reactive oxygen species in atmospheric aerosol containing quinoline components

Wenjun Zhang [a,c], Haoran Yu [b], Anusha Priyadarshani Silva Hettiyadura [a], Vishal Verma [b,**], Alexander Laskin [a,*]

[a] Department of Chemistry, Purdue University, West Lafayette, IN, 47907-2084, United States
[b] Department of Civil and Environmental Engineering, University of Illinois at Urbana–Champaign, Illinois, 61801, United States
[c] Key Laboratory of Integrated Regulation and Resources Development on Shallow Lakes of Ministry of Education, College of Environment, Hohai University, Nanjing, 210098, China

HIGHLIGHTS

- Ambient PM2.5 samples were collected in Midwest USA for quantitative analysis of their oxidative potential.
- The molecular composition of the PM2.5 samples was analyzed using advanced methods of high-resolution mass spectrometry.
- N-containing heterocyclic compounds enhance oxidative potential of PM2.5 organic components.

GRAPHICAL ABSTRACT

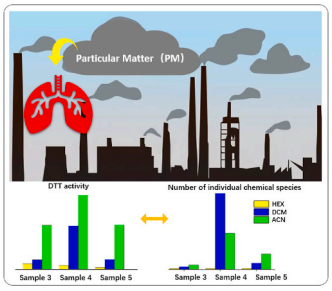

ABSTRACT

Organic constituents of atmospheric particular matter (PM) contribute significantly to prompt generation of reactive oxygen species (ROS) in particle phase, which is often quantified in terms of its oxidative potential (OP). In this study, we used complementary methods of the advanced molecular characterization and the OP quantitation to explore potential of different organic species to enhance ROS generation in ambient aerosol samples. We used seven $PM_{2.5}$ samples collected in the Midwest US, and extracted them sequentially into a set of solvents with different polarity: first non-polar hexane (HEX), then moderately polar dichloromethane (DCM) and finally polar deionized (DI) water. The DI extracts were further separated using solid phase extraction to isolate water-soluble organic carbon (WSOC) from inorganic ions. The OP of obtained extracts was analyzed using dithiothreitol (DTT) assay and reported here in terms of the DTT consumption rate (called DTT activity). The molecular composition of the same extracts was analyzed using a tandem platform of high-performance liquid chromatography (HPLC) coupled with a photodiode array detector (PDA) and a high-resolution mass spectrometer (HRMS). Highest DTT activities were observed in WSOC fractions (>1.1 μM min^{-1}) followed by DCM (0.75–1.1 μM min^{-1}) and HEX (<0.75 μM min^{-1}) fractions, respectively. These results were complemented by the HPLC-PDA-HRMS molecular characterization data indicating numerous redox-active polar organics detected in the WSOC fractions. In particular, chemical component with elemental formula of $C_{11}H_{11}N$ - attributed to dimethyl quinoline (DMQ) - was found systematically across all DTT-active fractions. The unprotonated nitrogen atom in the pyridine ring of quinolines facilitates electron transfer in the redox reactions, catalyzing generation of ROS in the quinoline containing samples. This is the first study that unambiguously identifies quinoline as a promoter of ROS generation determined within complex mixtures of ambient organic aerosols.

* Corresponding author.
** Corresponding author.
E-mail addresses: vverma@illinois.edu (V. Verma), alaskin@purdue.edu (A. Laskin).

https://doi.org/10.1016/j.atmosenv.2022.119406
Received 22 May 2022; Received in revised form 17 September 2022; Accepted 20 September 2022
Available online 1 October 2022

1. Introduction

Atmospheric aerosol is an inherent component of the air pollution associated with detrimental health effects, ranging from asthma and respiratory problems to cardiopulmonary disease and cancer (Pope et al., 1995a, 1995b; Dockery et al., 1993). One of the fundamental mechanisms causing the health effects is inhalation of aerosols that induce burst of reactive oxygen species (ROS) inside lung cells, exerting cellular oxidative stress (Oh et al., 2011; Karlsson et al., 2005). The ROS stand for a broad term that stands for a range of oxygen containing species with strong oxidizing abilities, such as superoxide anion ($O_2^{\bullet-}$), hydroxyl radical ($^{\bullet}OH$), hydrogen peroxide (H_2O_2) and other peroxides (See et al., 2007). Numerous studies have shown that various components of ambient particulate matter (PM) could catalyze the generation of ROS (Li et al., 2008; Garçon et al., 2006; Valavanidis et al., 2013). Thus, quantitative assessment of the ROS generation capability of specific molecular components of PM is a critical prerequisite necessary for predictive understanding of aerosol health effects. The ability of ambient particles to generate ROS (or consume physiological antioxidants) is conveniently called as the oxidative potential (OP) – an important metric related to environmental toxicity of the aerosol (Bates et al., 2019; Ayres et al., 2008).

There are several chemical methods to measure the OP in ambient PM samples, e.g., ascorbic acid (AA) assay (DiStefano et al., 2009), dithiothreitol (DTT) assay (Cho et al., 2005a), and measurement of ROS in a surrogate lung fluid (SLF) (Vidrio et al., 2009). Of these, the DTT assay is arguably the most commonly used method because of its sensitivity to many transition metals and aromatic organic compounds (Verma et al., 2015a). DTT assay is a cell-free chemical method developed for determining $O_2^{\bullet-}$ formation as the initial step in the generation of ROS (Delfino et al., 2013; Charrier and Anastasio, 2012). The consumption rate of DTT by PM samples has been found to be proportional to the particles' ability to induce a stress protein in cells (Fang et al., 2015). In this assay, redox-active substances in PM effectively catalyze the transfer of electrons from DTT to dissolved molecular oxygen, leading to the generation of $O_2^{\bullet-}$. The rate of DTT consumption is linked to the concentration of the redox-active substances in the sample (Li et al., 2009; Kumagai et al., 2002). Thus, DTT assay is used as a quantitative method to assess the capacity of PM samples to catalyze ROS generation. The particulate species responsible for DTT oxidation are typically examined by correlating DTT activity with PM chemical composition (Verma et al., 2014).

The variation of OP in PM is attributed to PM chemical composition, chemical-partition between PM and solution, solvent condition (pH (Li et al., 2022), dissolved oxygen, water vs. PBS vs. SLF, presence of proteins, surfactants, and antioxidants, etc.), and exact OP method (DTT concentration, incubation temperature, etc.) (Lin and Yu, 2019; Wei et al., 2020; Zhou et al., 2022). It was reported that transition metals or organic components elevate the OP, shown by the DTT assay measurments (Verma et al., 2015a; Fang et al., 2015). Among the soluble transition metals of $PM_{2.5}$, Copper and Manganese are the most DTT-active (Charrier and Anastasio, 2012; Yu et al., 2018). Some inorganic ions, such as SO_4^{2-}, NO_3^- and NH_4^+ are also moderately associated with DTT activity (Wang et al., 2018). Selected organic species such as quinones have been also identified as the major DTT active components in PM (Yiqiu et al., 2018; Tuet et al., 2017).

Humic-like substances (HULIS), a complex mixture of large molecular weight compounds containing aromatic moieties (of which quinones and hydroxyquinones are a subset) have been known as major redox-active components of water-soluble organic carbon (WSOC) (Verma et al., 2012, 2015a; Lin and Yu, 2011). HULIS are components of light absorbing organic aerosols (OA), also known as brown carbon (BrC) (Verma et al., 2015a). Laboratory studies indicated that while reduced N-containing organic bases such as pyridine, imidazole and their alkyl derivatives show no redox activity on their own, their complexation with HULIS enhances redox activity of quinones (modeled with 1,4-naphthoquinone standard) and therefore WSOC (Dou et al., 2015). This enhancement is proportional to the amount of N-containing organic bases in the assay solutions, which was attributed to ability of the unprotonated N atom to act as a H-bonding acceptor, facilitating hydrogen-atom transfer in the ROS generation cycle (Dou et al., 2015). Considering complexity of organic components in ambient PM samples and broad range of their individual species (of which only a fraction is typically speciated), an explicit detection of organic components with strong catalytic effects on the ROS generation is largely lacking (Verma et al., 2015a). Thus, there is a clear need to develop and apply molecular-specific methods to identify and characterize the organic compounds that enhance ROS generation in ambient aerosol, deciphering their direct and catalytic effects on ROS.

In this work, we utilize high performance liquid chromatography (HPLC) separation coupled with photodiode array (PDA) and high resolution mass spectrometry (HRMS) detection that has been used in our previous work, (Lin et al., 2015a,b) in conjunction with DTT assay to identify ROS active components of $PM_{2.5}$ for the first time. Additional insights to the compound class specific ROS activity is provided through analysis of sequentially extracted $PM_{2.5}$ using a suite of non-polar and polar solvents.

2. Methods and materials

2.1. Ambient $PM_{2.5}$ sampling and solvent extractions

Seven ambient $PM_{2.5}$ samples were collected in January–April 2017 from the roof of Newmark Civil and Environmental Engineering building of UIUC (Urbana, IL; height from the ground level 30 m) using a high-volume sampler (flow rate = 1.13 m^3/min) with a $PM_{2.5}$ inlet (Tisch Environmental; Cleves, OH). Detail of the sampling site has been provided elsewhere (Yu et al., 2018). Briefly, the site is 240 m south of a major street (University Avenue) and is approximately 1 km from downtown Champaign. Therefore, the major emission sources at the site are vehicular emissions along with resuspended local dust. In addition to these local sources, the sampling site is probably impacted by the long-range transported pollution coming from northwest (for sample 3 and 5) and southern regions (for sample 4), as indicated by the backward air mass trajectories on different sampling dates (Fig. S1).

Prebaked 8 × 10 in. quartz filters (Pallflex Tissuquartz, Pall Life Sciences; Port Washington, NY) were used for sample collection. Each sample was collected for a period of 72 h. Sample collection information, including the sampling period and estimated $PM_{2.5}$ mass loading on each filter, is listed in Table S1. After sample collection, the filters were immediately wrapped in aluminum foil, sealed and stored in a freezer at −20 °C until analyses. Two field blanks were collected by leaving blank filters in the filter holder at the sampling site for 5 min, but without turning on the pump. The meteorological parameters as obtained from the University of Illinois – Willard Airport station (8 km southwest of the sampling site) are also shown in Table S1. The average temperature and relative humidity (RH) at the sampling site during the whole sampling period were 9.5 ± 6.4 °C and 66.9 ± 12.6 %RH, respectively, indicating stable meteorological conditions throughout all the samples. The prevailing wind was generally from south or west. Therefore, the emissions from residential heating and business developments from urban area of Champaign city (1 km southwest of the sampling site) are also expected.

Fig. 1 shows schematics indicating sequence of solvent extraction steps and modes of the chemical analysis employed for each of the fractionated samples. Five punches (1" diameter) of quartz filters with ambient $PM_{2.5}$ samples were extracted into 10 mL of hexane (HEX), dichloromethane (DCM) and deionized water (DI; Milli-Q; resistivity = 18.2 MΩ/cm) stepwise, in the sequence of increasing polarity. After the final step of extraction, the DI extracts were fractionated using solid phase extraction (SPE) on C18 cartridges to separate hydrophobic WSOC from inorganic ions (effluent). The DI extracts were acidified prior SPE

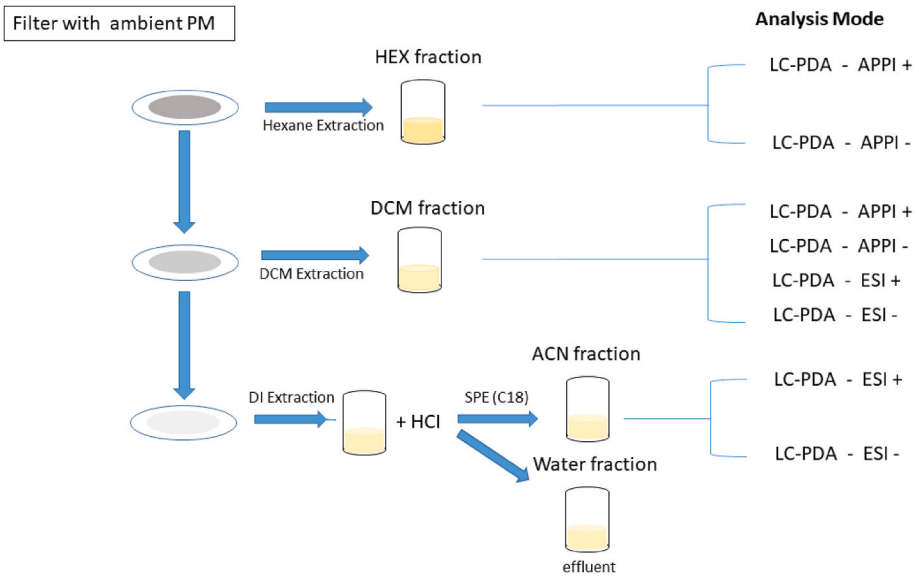

Fig. 1. Sequential steps of ambient $PM_{2.5}$ extraction into solvents with increasing polarity ($P_{HEX} = 0.1$, $P_{DCM} = 0.31$, $P_{ACN} = 0.58$, $P_{water} = 1.0$) and modes of the chemical analysis employed for each of the fractionated samples. Detailed inventory of all analyzed samples is included in Table S1.

using hydrochloric acid (HCl) until the solution reached pH = 2 to promote retention of acidic OA in C18 cartridges. The retained fraction on C18 cartridge was eluted with 10 mL acetonitrile (ACN). Afterwards, organic solvent (i.e., HEX, DCM and ACN) extracts were evaporated down to a volume of 100 μL, separately, under a very light stream of ultra-pure nitrogen gas, and the residuals were reconstituted into 5 mL DI for the DTT assay. In order to increase the miscibility, 100 μL dimethylsulfoxide (DMSO) was added into HEX and DCM extracts prior to reconstitution. Blank filters were extracted following the same procedure described above to eliminate the interference of background.

2.2. DTT assay

The fractions extracted in organic solvents and reconstituted in DI were analyzed for DTT activity using an automated DTT system (Yu et al., 2018). Briefly, a mixture containing 3.5 mL sample extraction, 1 mL of 0.5 mM potassium phosphate buffer (K-PB, pH = 7.4, pretreated with Chelex column to remove the trace metals), and 0.5 mL of 1 mM DTT were added into the reaction vial kept in a thermomixer (550 rpm and 37 °C). At fixed reaction time points of 3, 15, 27, 39, and 51 min, we withdrew 100 μL aliquots of the reaction mixture and mixed them with 500 μL of 200 μM 5,5′-dithiobis-(2-nitrobenzoic acid) (DTNB), which reacts with DTT and produces a yellow-colored complex 2-nitro-5-thiobenzoic acid (TNB). After further dilution of the mixture with DI, the absorbance of the TNB complex is measured at its characteristic 412 nm wavelength by a liquid waveguide capillary cell (LWCC; World Precision Instruments; Sarasota, FL) coupled with an online flame miniature spectrophotometer (Ocean Optics; Dunedin, FL, US) and an ultraviolet–visible–near-infrared (UV–vis–NIR) light source. The consumption rate of DTT (i.e. DTT activity, μM/min) was determined as the slope of the linear regression of DTT concentration versus reaction time. To ensure the stability of DTT assay, we used 0.25 μM phenanthrenequinone (PQ) as the positive control. The tests of positive control were conducted every 10 samples, and the blank-corrected DTT activity of 0.25 μM PQ was 2.0 ± 0.05 μM min^{-1}, indicating a strong robustness of the DTT assay protocol.

2.3. HPLC-PDA-HRMS analysis

Chemical speciation of organic constituents of ambient $PM_{2.5}$ samples extracted in to ACN (polarity index 0.58), DCM (polarity index 0.31) and HEX (polarity index 0.1) extracts were analyzed using HPLC-PDA-HRMS platform assisted with either dopant-assisted atmospheric pressure photoionization (APPI) or electrospray ionization (ESI) sources operated in positive and negative modes, as illustrated in Fig. 1. Application of complementary ESI and APPI sources and data acquisition in both polarity modes are essential for comprehensive analysis of complex OA mixtures. The details of instruments and measurement procedures are published elsewhere (Lin et al., 2018). Briefly, the separation was performed on a reversed-phase column (Luna C18, 2 × 150 mm^2, 5 μm particles, 100 Å pores, Phenomenex, Inc.). The binary mobile phases included: (A) water with 0.1% v/v formic acid (LC/MS grade, Fisher chemical) and (B) ultrapure grade acetonitrile with 0.1% v/v formic acid (LC/MS grade, Fisher chemical). A stepwise gradient elution was performed at a flow rate of 200 μL/min: 0–5 min hold at 90% A, 5–85 min linear gradient to 10% A, 85−86min linear gradient to 0% A, 86–94 min hold at 0% A, 94–95 min linear gradient to 90% A and then 95–120 min hold at 90% A to recondition the column for the next sample. UV–vis absorption spectra were measured using the PDA detector over the wavelength range of 200–680 nm.

Considering that there were predominantly polar and non-polar compounds in ACN and HEX fractions, respectively, ESI was used to analyze ACN fractions and APPI was used to analyze HEX fractions. Both ESI and APPI were used to analyze DCM fractions that contain moderately polar OA. The ESI settings used were a spray voltage of 3.5 kV in both positive and negative ion modes, 250 °C capillary temperature, 35 units of sheath gas flow, 10 units of auxiliary gas flow, and 1 units of sweep gas flow. The APPI settings used were a spray voltage of 5 kV in both positive and negative ion mode, 225 °C capillary temperature, 400 °C vaporizer temperature, 35 units of sheath gas flow, 10 units of auxiliary gas flow, and 0 units of sweep gas flow. A mixture of 3-(trifluoromethyl) anisole (TFMA) and chlorobenzene (1:99 v/v) was used as the dopant in APPI to promote proton transfer and charge exchange reactions. The dopant was injected by a syringe pump at a flow rate of 20 μL/min and was mixed with the mobile phase after exiting the column and before entering the ion source using a tee adaptor. HRMS spectra were acquired for a mass range 80–1200 Da, at mass resolving power of 240,000 at m/z 200.

2.4. Data analysis

The HPLC-PDA-HRMS data were acquired and processed by Xcalibur

(Thermo Scientific) software and peak detection in LC-MS data were performed using an open source software toolbox, MZmine 2 (http://mzmine.github.io/). Pluskal et al. (2010) detected peaks in our samples were not considered if the same peaks were detected in blanks and their intensity ratios (peak height in samples/peak height in blanks) were less than 10. Molecular formulas were assigned using MIDAS molecular formula calculator (http://magnet.fsu.edu/~midas/download.html) which employs valence rules. Formula assignments were assisted with the Kendrick mass defect grouping of MS features using a suite of Microsoft Excel macros developed in our group (Lin et al., 2018). Assignments were restricted by ±2 ppm mass accuracy filter and by the following constraints of elemental composition: C ≤ 100, H ≤ 200, N ≤ 3, O ≤ 50, S ≤ 1, and Na ≤ 1 (positive mode only). ESI (+) assignments assumed $[M+H]^+$ and $[M+Na]^+$ ions; APPI (+) assumed $[M+H]^+$ and $M^{\bullet+}$ ions; ESI (−) and APPI (−) assumed [M-H]- ions. Based on these restrictions, >70% of the considered peaks were assigned with elemental formulas in each of the samples. Neutral formulas corresponding to ions detected in positive and negative modes were calculated, respectively. Double-bond equivalent (DBE) for the neutral formulas were calculated according to equation: DBE = c − h/2 + n/2 + 1, where c, h, and n are referred to the number of carbon, hydrogen, and nitrogen atoms in the neutral formula (McLafferty and Tureček, 1993).

3. Results and discussion

3.1. DTT activity

Fig. 2A shows DTT activity measured in each of the solvent extracted sample fractions. DTT activity in ACN fractions was significantly higher than that of DCM and HEX fractions in all of the PM samples. Sample 4 shows the highest DTT activity in both DCM and ACN fractions. DTT activities of other HEX and DCM extracts were only slightly above the blank levels (0.76 ± 0.06 μM min^{-1}). Thus, we conclude that WSOC and moderately-polar organic constituents have a larger influence on ROS generation than non-polar organics extracted into HEX, which was consistent with previous findings. For instance, Verma et al. (2015b) observed that the methanol extracted OA possessed most of the DTT activity (>70%), followed by DCM fraction (median = 9%), while the HEX fraction had the least activity (<5%). Similarly, Li et al. (2000) also found polar compounds eluted with 1:1 DCM: methanol mixture (v/v) in DCM extracted diesel exhaust particles induce the highest heme oxygenase-1 (HO-1) expression, possessing an excellent correlation with DTT activity in RAW264.7 cells. Overall, these results indicate that polar to moderately polar OA play an important role in ROS generation.

3.2. Chemical characterization

Fig. 2B shows the number of individual chemical species identified in each of the analyzed solvent-extracted samples. Number of the detected species in DCM and ACN fractions was significantly higher than that in HEX fraction, particularly in sample 4. More compounds were detected in sample 4 than in samples 3 and 5. This suggest that WSOC contains more compounds that are either redox active or promote ROS generation, which is consistent with previous literature reports (Lin and Yu, 2011; Verma et al., 2012; Cao et al., 2021) Examples of compounds detected in explicitly in the ACN extracts of WSOC include: $C_7H_8O_3$ (RT = 9.4 min), $C_9H_6O_3$ (RT = 21.6 min), $C_8H_{12}O_6$ (RT = 9.3 min), $C_{12}H_{21}NO_3$ (RT = 37.8 min) and $C_8H_{16}O_6$ (RT = 5.7 min). $C_7H_8O_3$ could be salicylic acid, which is a known plant defense regulator (Csiszár et al., 2018). $C_9H_6O_3$ could be the umbelliferon, a phenolic compound, and therefore is a potential antioxidant (Vandana et al., 2014). $C_8H_{12}O_6$ could be 3-O-ethylascorbic acid, a radical scavenger (Tai et al., 2014). $C_{12}H_{21}NO_3$ could be fuchsisenecionine, which is an alkaloid that can participate in oxidation-reduction reactions (Leonard and Manske, 1960). Compounds detected in all 3 samples in different fractions were collectively assessed. The identified formulas in each fraction were further classified into five major compound categories based on their elemental composition: CH, CHO, CHN, CHON, CHOS and CHONS. Accordingly, CHON refers to the compounds that contain carbon, hydrogen, oxygen, and nitrogen elements. Other compound categories are defined analogously. The sulfur (S)-containing compounds were found as both CHOS (11.1% of S compounds detected in all 3 fractions) and CHONS (88.9% of S compounds detected in all 3 fractions) composition. Fig. 3 displays summary of the identified species in ACN and DCM fractions based on the HR-MS peak assignments, combining experimental results obtained in all (±)APPI and (±)ESI modes (summary of all identified chemical components is included in the SI file HRMS data.xlsx). HEX fraction is not shown in Fig. 3 due to very few detected species. For DCM and ACN fractions, CHO was the most abundant category observed by both APPI and ESI, followed by CHON and CHN. (+)ESI detects an overwhelmingly large number of compounds compared with other ionization modes.

Fig. 4 shows a plot of DBE versus Carbon number, which is used to identify potential ROS-active BrC species that contain extensive network of π-bonds and are mapped by the blue shaded area (Daher et al., 2014). This area includes: N-containing aromatic N-heterocyclic compounds, $C_{12}H_{13}N$ and $C_{11}H_{11}N$ and other N- and O-containing aromatic compounds that are tentatively assigned as either oxygenated PAHs, carboxylic acid containing aromatics or phenolics containing aliphatic chains, $C_7H_8O_4$, $C_7H_8O_3$, $C_8H_6O_2$, $C_8H_{10}O$, $C_9H_{10}O_2$, $C_9H_6O_3$, $C_{10}H_6O_2$, $C_{10}H_8O_2$, $C_{11}H_{12}O$, $C_{11}H_4O$, $C_{12}H_6O_2$, $C_{12}H_{14}O_4$, $C_{15}H_{10}O_6$, $C_9H_9NO_4$, $C_{10}H_9NO_4$, $C_{10}H_{13}NO_3$, $C_9H_5NO_5$, $C_{20}H_{24}N_2O_5$, and $C_{10}H_7NO_3$. Based on retention times and DBE, the compounds with the formula $C_{11}H_{11}N$ and $C_{12}H_{13}N$ were tentatively identified as quinolines (Xia et al., 2016), discussed in the next section. Similarly, $C_9H_9NO_4$, $C_{10}H_8O_2$, $C_{10}H_9NO_4$ and $C_{15}H_{10}O_6$ detected in this area were tentatively identified as

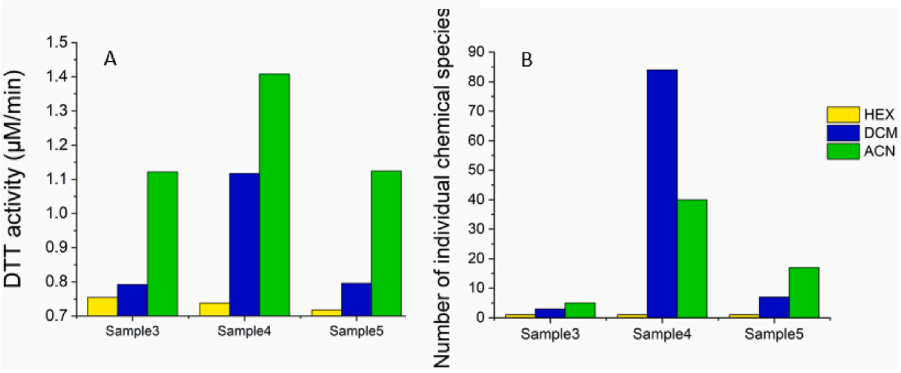

Fig. 2. A) Results of DTT activity (μM/min) after blank correction; B) Number of individual chemical species identified in each of the samples and their fractions. Samples 1 and 2 were field blank filters.

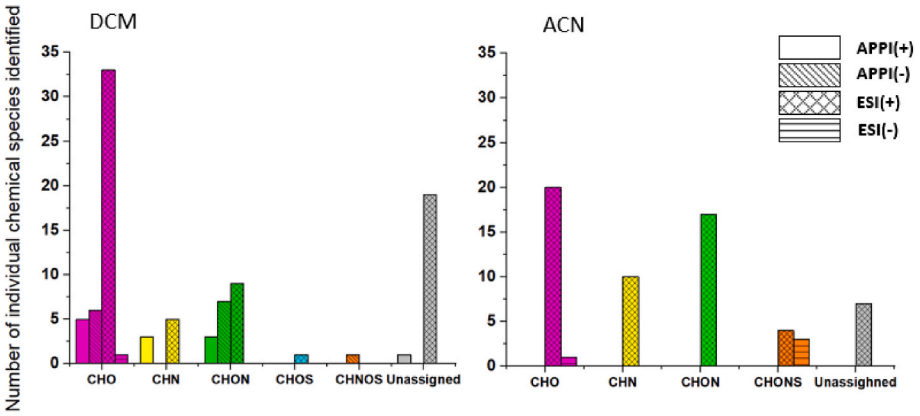

Fig. 3. Histogram of number of elemental formulas detected in each of the listed chemical classes identified in DCM and ACN fractions of sample 3, 4 and 5 in ESI and APPI modes.

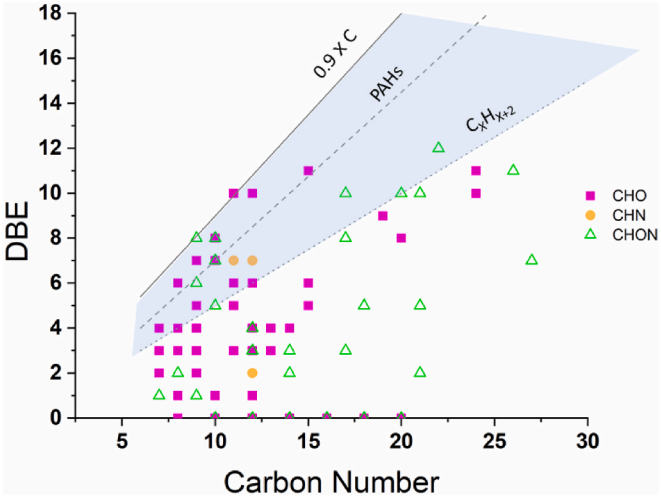

Fig. 4. Plot of the double bond equivalent (DBE) vs number of carbon atoms in assigned species. Black lines indicate DBE reference values of linear conjugated polyenes C_xH_{x+2}, characterized by DBE = 0.5 × C (dotted line), cata-condensed PAHs with DBE = 0.75 × C - 0.5 (intermittent line), and fullerene-like hydrocarbons with DBE = 0.9 × C (solid line). Data points inside the blue shaded area are potentially ROS-active aromatic species. (For interpretation of the references to color in this figure legend, the reader is referred to the Web version of this article.)

oxygenated PAHs. Similar N-containing aromatic species are commonly reported in the biomass burning organic aerosols (BBOA) (Laskin et al., 2009), which is plausibly related to the rural residential heating in the area of our study Previous studies showed that PAHs often strongly correlate with DTT activity, but PAHs are not redox active (Cho et al., 2005a; Shirmohammadi et al., 2017; Jin et al., 2019; Saffari et al., 2014). It is therefore believed that their correlation with DTT loss is due to a correlation between PAHs and quinones, as quinones can derive from oxidation of PAHs (Cho et al., 2005b). Accordingly, $C_{10}H_6O_2$ and $C_{10}H_8O_2$ were likely quinones. Some aromatic compounds that contain aliphatic chains with carboxylic groups were detected in our samples, those include $C_9H_6O_3$, $C_9H_9NO_4$, $C_{10}H_{13}NO_3$, $C_9H_5NO_5$, $C_{10}H_9NO_4$ and $C_{20}H_{24}N_2O_5$. We also found aromatic compounds that contain aliphatic chains with phenol terminal groups, including $C_8H_{10}O$, $C_{10}H_7NO_3$ and $C_{15}H_{10}O_6$ (Krivacsy et al., 2000; Kiss et al., 2002). Overall these results indicate that WSOC components have significant influence on ROS generation.

3.3. Identification of $C_{11}H_{11}N$

$C_{11}H_{11}N$ ($m/z = 158.0965$) was found across all DTT-active fractions (i.e. 3 ACN fractions and sample 4 DCM fraction). Because it was detected in positive ionization mode and its DBE was 7, we inferred that it might be a N-heterocyclic compound. Considering that it is also detected in the potential aromatic region (Fig. 4), it is likely an N-containing heterocyclic compound with two fused aromatic rings. Structure of this $C_{11}H_{11}N$ compound is identified as an isomer of dimethylquinoline based on HPLC-PDA-ESI(+)-HRMS (Pope et al., 1995b) analysis of available dimethylquinoline (DMQ) commercial standards (2,6-DMQ, 98% pure, Sigma-Aldrich; 2,8-DMQ,B; 95% pure, Sigma-Aldrich; 3, 4-DMQ, ≤100% pure, Sigma-Aldrich) and $C_{11}H_{11}N$ species found in the DTT active fractions. Fig. 5 shows comparison of the MS (Pope et al., 1995b) fragmentation spectra of three DMQ standards and the $C_{11}H_{11}N$ experimental analyte. For each of the species, MS (Pope et al., 1995b) spectra were acquired and averaged during their respective elution time windows. All four spectra show remarkable similarity in the fragmentation patterns of analytes, indicating closely related DMQ molecular structures. However, exact elution time of $C_{11}H_{11}N$ detected in the sample was different from the standards (Fig. S2), suggesting an additional isomer with alternatively arranged methyl groups, for which commercial standard was not found. Hereafter, we call experimental $C_{11}H_{11}N$ species as DMQ*, whereas an asterisk symbol indicates that exact location of its two methyl groups is unknown. Assumption of the DMQ* isomer (rather than other molecular structures) is further supported by similarity of the UV–vis spectra (Fig. S3; common 300–320 nm absorption band). Based on the DMQ* assignment and assuming the 2, 8-DMQ intensity vs mass calibration values, we estimate the concentration of DMQ* in the ACN fraction of sample 3 at the level of 1.7 μg/L and thereby the estimated ambient concentration of DMQ* in $PM_{2.5}$ is ~0.057 ng/m^3 (Appendix A, SI file).

3.4. Catalytic role of DMQ

It has been reported that redox-active HULIS components of WSOC promote ROS generation, where HULIS serve as electron carriers (Lin and Yu, 2011). Reaction Scheme 1 summarizes the mechanism of DMQ*-promoted ROS generation adopted from Dou et al. (2015), illustrated together with the concomitant DTT assay reaction chemistry. Notably, Dou et al. reported that nitrogen-containing organic bases, such as pyridine, imidazole and their alkyl derivatives, show no DTT activity on their own, but they catalytically promote ROS generation in the presence of HULIS (Dou et al., 2015). Their catalytic activity is attributed to unprotonated N atoms acting as an H-bonding acceptors that therefore facilitate proton/electron transfer of redox active compounds such as quinone (Dou et al., 2015). DMQ* is an N-containing

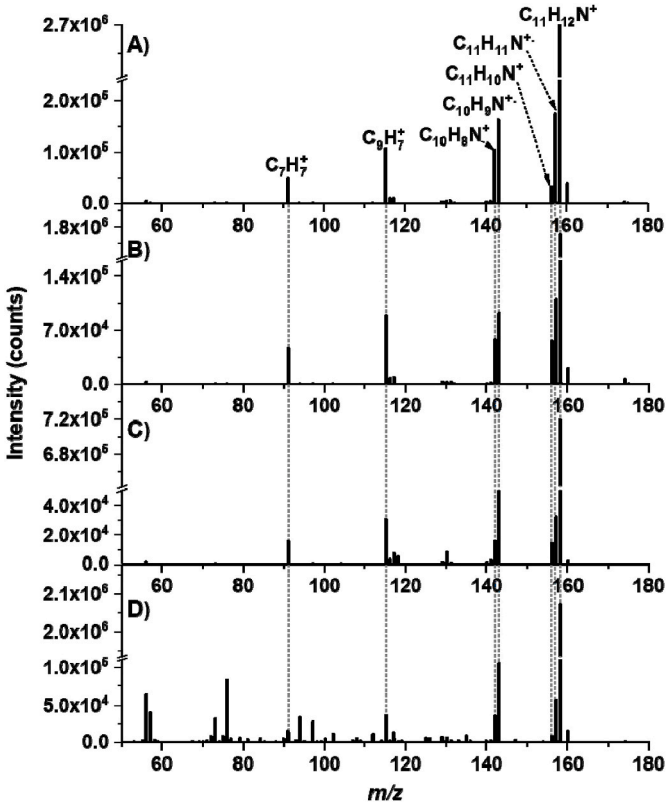

Fig. 5. The MS (Pope et al., 1995b) spectra of m/z 158 $[C_{11}H_{11}N + H]^+$ corresponding to standards of A) 2,6-dimethylquinoline, B) 2,8-dimethylquinoline, C) 3,4-dimethylquinoline compared to C) the same m/z 158 species detected in the DTT active fractions (ACN fraction of sample 1 is shown here). Dashed lines indicate 6 common abundant fragment ions and the parent ion detected in all four MS (Pope et al., 1995b) spectra.

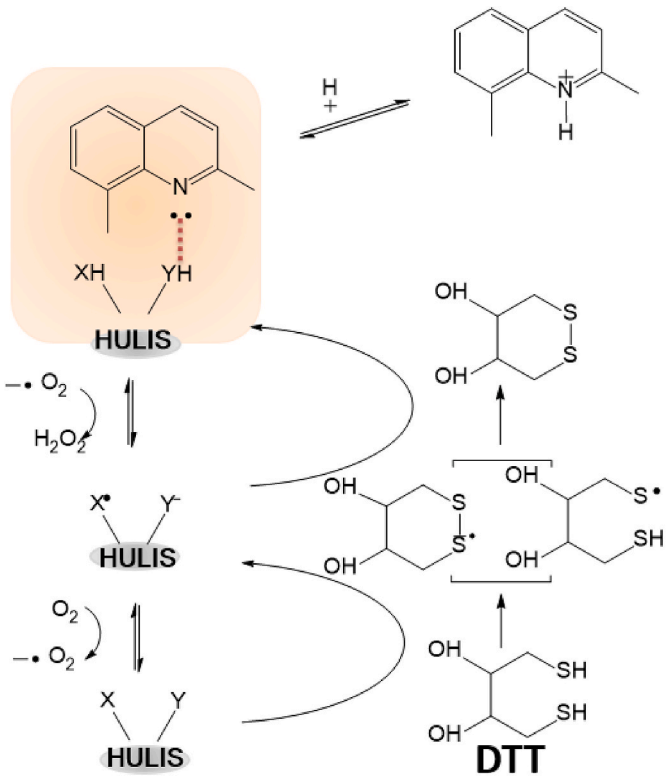

Reaction Scheme 1. Conceptual diagram of HULIS-catalyzed ROS production and concomitant consumption of DTT, with DMQ* (dimethyl quinoline compounds, illustrated as an 2,8-DMQ isomer) facilitating the oxidation of HULIS through H-bonding (highlighted by the orange shaded area) adopted from by Dou et al. (2015)

aromatic heterocyclic compound, thus it is expected to promote the ROS generation by facilitating proton/electron transfer of redox active compounds similar to the previously studied single-ring pyridine and imidazole (Dou et al., 2015).

In our study, $C_{11}H_{11}N$ (DMQ*) was identified as a common feature across all DTT active fractions. This compound belongs to the class of alkaloids, similar to pyridine, imidazole and their alkyl derivatives, and it is likely a product of biofuel burning (Laskin et al., 2009). Commonly for the alkaloids detection (Lin et al., 2012), DMQ* was observed under positive electrospray ionization mode in the HULIS fraction of ambient samples. More importantly, it contains an unprotonated N atom. Based on the above similarities, we infer that DMQ* could promote ROS generation in the presence of HULIS similar to pyridine (Dou et al., 2015), imidazole (Dou et al., 2015), imidazole-2-carboxaldehyde, and 1N-glyoxal-substituted imidazole (Sedehi et al., 2013; Haan et al., 2009, 2011).

Moreover, Dou et al. (2015) found that the ROS activity of HULIS enhanced by nitrogen-containing bases was increased with their increased levels in the DTT assay solutions. To confirm that DMQ could enhance catalytic effect of redox-active compounds in ROS generation, we spiked the DTT solution with 2,8-DMQ at different concentrations (2–300 ppb). Due to limited mass loadings on the filters, we could not conduct the interaction experiments for each sample at all tested concentrations of 2,8-DMQ. Specifically, the HULIS fractions extracted from samples 3, 4 and 5 was used to study the interactions at higher concentrations of 2,8-DMQ (i.e., 20–300 ppb), while samples 6, 7, 8 and 9 were used to test the interactions at lower concentrations (i.e., 2–10 ppb of 2,8-DMQ).

Overall, 2,8-DMQ itself did not show any DTT activity compared to the blanks (Fig. S4), which is consistent with earlier report of Dou et al. (2015) However, significant interactions were observed between HULIS and 2,8-DMQ, at different concentrations. Fig. 6 shows the interaction factor (IF) of HULIS fractions from DCM and ACN extractions with different concentrations of 2,8-DMQ. Since the DTT activity of 2,8-DMQ was equal to the blank level at all concentrations, *IF* is defined as the ratio of the DTT activity of sample spiked with 2,8-DMQ over the DTT activity of the unspiked sample (Yu et al., 2018). $IF > 1$ indicates an enhancement effect of 2,8-DMQ to the DTT activity of the spiked $PM_{2.5}$ extract. None of the HEX fractions spiked with 2,8-DMQ show a clear trend of DTT activity even with the substantial increase of 2,8-DMQ concentration up to 300 ppb (Fig. S5). In contrast, ACN and DCM fractions showed substantially higher DTT activity when spiked with 2–10 ppb of 2,8-DMQ. Strong synergistic interaction between DCM extracts and 2,8-DMQ is observed (IF = 1.2–4), while the interaction between ACN extracts and 2,8-DMQ is generally additive (IF = 0.8–1.2). On further increasing the concentration of 2,8-DMQ (i.e., 200–300 ppb), we clearly observed a substantial increase in IFs for DCM extracts (IF = 3.0–4.8). ACN fraction in sample 5 showed the strongest synergistic interaction with 2,8-DMQ (concentration range: 20–100 ppb) in DTT activity among all fractions (IF up to 10). Although these results do not indicate a linear trend of DTT activity with the increase of DMQ concentration, an increase of DTT activity was observed in most samples and fractions upon spiking with 2,8-DMQ, including those that initially (or originally) did not show any DTT activity. Thus, these results indicate that 2,8-DMQ enhances the catalytic effect of redox-active compounds in ROS generation.

3.5. Environmental implications

Our results indicate that N-containing heterocyclic compounds

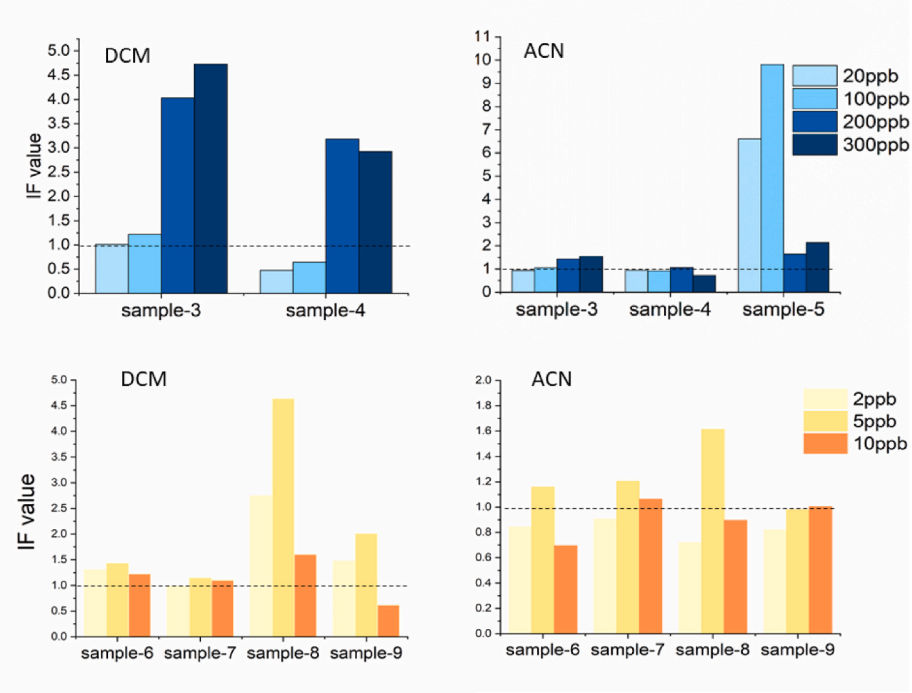

Fig. 6. Interaction factor (*IF*) calculated for DCM and ACN fractions in the $PM_{2.5}$ samples at different spiked concentrations of 2,8-DMQ. $IF > 1$ indicates a synergistic interaction. DTT activities of S5-DCM with or without 2,8-DMQ were below detection limit. Line at 1.0 to indicate the threshold of synergistic interaction.

enhance ROS generation by OA components. Presuming ROS as a health-relevant metric, it implies that the ambient samples containing both N-containing aromatic heterocycles and redox-active WSOC compounds will exert a greater impact on human health than redox active organic compounds alone (Dou et al., 2015). Similarly, compounds containing H-bond acceptors, such as N-containing heterocycles that are non-aromatic, alkyl amines, dioxane, pyran, and thiols, might exert the same effect as N-containing aromatic heterocycles, which has not been investigated yet. Therefore, to fully evaluate the ROS activity of PM, it is necessary to identify the other H-bond acceptors in PM and determining their role in ROS generation. Previous studies have detected quinolines, and pyridines in atmospheric samples. Cooked meat and tobacco smoke are the major sources of heterocyclic aromatic amines with multiple rings and N-heteroatoms (Guy et al., 2000). N-containing aromatic heterocycles were also detected in tobacco smoke and in fossil fuel combustion emissions (Chen and Preston, 1998). Crop residue burning, a very common and widespread type of open burning in Southeast Asia, especially in China and India, is reported as the major source of N-containing heterocycles (Laskin et al., 2009; Claeys et al., 2012; Ma and Hays, 2008; Samy et al., 2013). Moreover, ROS generation by PM could also be enhanced by histidine residues containing N-bases in human bodies (Dou et al., 2015). A comprehensive understanding of the relationships between PM constituents and related ROS activity could help to inform public health managements and mitigation policies related to the PM pollution. Admittedly, the small sample size and the limited filter sections available for this study did not allow us to conduct repeated measurements for different experimental conditions. These limits of our study restrict broader interpretation of the observed results and their environmental implications for assessing more complex interactions among PM components emitted from diverse sources. Therefore, more systematic studies with larger sample size are needed to evaluate the levels of N-heterocyclic constituents in ambient samples as well as pinpoint their roles on the health effects of PM.

CRediT authorship contribution statement

Wenjun Zhang: Formal analysis, Writing – review & editing, performed the HPLC–HRMS measurements and analyzed the data, integrated the experimental datasets and led manuscript preparation, all authors contributed its review and editing. **Haoran Yu:** Writing – review & editing, performed the OP measurements, integrated the experimental datasets and led manuscript preparation, all authors contributed its review and editing. **Anusha Priyadarshani Silva Hettiyadura:** Formal analysis, Writing – review & editing, performed the HPLC–HRMS measurements and analyzed the data. all authors contributed its review and editing. **Vishal Verma:** Conceptualization, Formal analysis, Methodology, Writing – review & editing, conceptualized the experiments and analytical methodologies of the study, secured grant support for this study and managed the project, all authors contributed its review and editing. **Alexander Laskin:** Conceptualization, Formal analysis, Methodology, Writing – review & editing, conceptualized the experiments and analytical methodologies of the study, secured grant support for this study and managed the project, all authors contributed its review and editing.

Declaration of competing interest

The authors declare that they have no known competing financial interests or personal relationships that could have appeared to influence the work reported in this paper.

Data availability

Data will be made available on request.

Acknowledgments

The UIUC group acknowledges support from Vishal Verma's startup fund by the Department of Civil and Environmental Engineering at University of Illinois at Urbana-Champaign, and partial support from the National Science Foundation award CBET-1847237. The Purdue group acknowledges support from the Purdue Climate Change Research Center and partial support from the National Science Foundation award CBET-2107946. Wenjun Zhang acknowledges support from the China

Scholarship Council.

Appendix A. Supplementary data

Supplementary data to this article can be found online at https://doi.org/10.1016/j.atmosenv.2022.119406.

References

Ayres, J.G., Borm, P., Cassee, F.R., Castranova, V., Donaldson, K., Ghio, A., Harrison, R. M., Hider, R., Kelly, F., Kooter, I.M., Marano, F., Maynard, R.L., Mudway, I., Nel, A., Sioutas, C., Smith, S., Baeza-Squiban, A., Cho, A., Duggan, S., Froines, J., 2008. Evaluating the toxicity of airborne particulate matter and nanoparticles by measuring oxidative stress potential—a workshop report and consensus statement. Inhal. Toxicol. 20 (1), 75–99.

Bates, J.T., Fang, T., Verma, V., Zeng, L., Weber, R.J., Tolbert, P.E., Abrams, J.Y., Sarnat, S.E., Klein, M., Mulholland, J.A., Russell, A.G., 2019. Review of acellular assays of ambient particulate matter oxidative potential: methods and relationships with composition, sources, and health effects. Environ. Sci. Technol. 53 (8), 4003–4019.

Cao, T., Li, M., Zou, C., Fan, X., Song, J., Jia, W., Yu, C., Yu, Z., Peng, P.a., 2021. Chemical composition, optical properties, and oxidative potential of water-and methanol-soluble organic compounds emitted from the combustion of biomass materials and coal. Atmos. Chem. Phys. 21 (17), 13187–13205.

Charrier, J., Anastasio, C., 2012. On dithiothreitol (DTT) as a measure of oxidative potential for ambient particles: evidence for the importance of soluble transition metals. Atmos. Chem. Phys. 12 (5), 11317.

Chen, H.-Y., Preston, M.R., 1998. Azaarenes in the aerosol of an urban atmosphere. Environ. Sci. Technol. 32 (5), 577–583.

Cho, A.K., Sioutas, C., Miguel, A.H., Kumagai, Y., Schmitz, D.A., Singh, M., Eiguren-Fernandez, A., Froines, J.R., 2005a. Redox activity of airborne particulate matter at different sites in the Los Angeles Basin. Environ. Res. 99 (1), 40–47.

Cho, A.K., Sioutas, C., Miguel, A.H., Kumagai, Y., Froines, J.R., 2005b. Redox activity of airborne particulate matter (PM) at different sites in the Los Angeles Basin. Environ. Res. 99 (1), 40–47.

Claeys, M., Vermeylen, R., Yasmeen, F., Gómez-González, Y., Chi, X., Maenhaut, W., Mészáros, T., Salma, I., 2012. Chemical characterisation of humic-like substances from urban, rural and tropical biomass burning environments using liquid chromatography with UV/vis photodiode array detection and electrospray ionisation mass spectrometry. Environ. Chem. 9 (3), 273–284.

Csiszár, J., Brunner, S., Horváth, E., Bela, K., Ködmön, P., Riyazuddin, R., Gallé, Á., Hurton, Á., Papdi, C., Szabados, L., 2018. Exogenously applied salicylic acid maintains redox homeostasis in salt-stressed Arabidopsis gr1 mutants expressing cytosolic roGFP1. Plant Growth Regul. 86 (2), 181–194.

Daher, N., Saliba, N.A., Shihadeh, A.L., Jaafar, M., Baalbaki, R., Shafer, M.M., Schauer, J. J., Sioutas, C., 2014. Oxidative potential and chemical speciation of size-resolved particulate matter (PM) at near-freeway and urban background sites in the greater Beirut area. Sci. Total Environ. 470, 417–426.

Delfino, R.J., Staimer, N., Tjoa, T., Gillen, D.L., Schauer, J.J., Shafer, M.M., 2013. Airway inflammation and oxidative potential of air pollutant particles in a pediatric asthma panel. J. Expo. Sci. Environ. Epidemiol. 23 (5), 466.

DiStefano, E., Eiguren-Fernandez, A., Delfino, R.J., Sioutas, C., Froines, J.R., Cho, A.K., 2009. Determination of metal-based hydroxyl radical generating capacity of ambient and diesel exhaust particles. Inhal. Toxicol. 21 (9), 731–738.

Dockery, D.W., Pope, C.A., Xu, X., Spengler, J.D., Ware, J.H., Fay, M.E., Ferris Jr., B.G., Speizer, F.E., 1993. An association between air pollution and mortality in six US cities. N. Engl. J. Med. 329 (24), 1753–1759.

Dou, J., Lin, P., Kuang, B.-Y., Yu, J.Z., 2015. Reactive oxygen species production mediated by humic-like substances in atmospheric aerosols: enhancement effects by pyridine, imidazole, and their derivatives. Environ. Sci. Technol. 49 (11), 6457–6465.

Fang, T., Verma, V., Guo, H., King, L., Edgerton, E., Weber, R., 2015. A semi-automated system for quantifying the oxidative potential of ambient particles in aqueous extracts using the dithiothreitol (DTT) assay: results from the Southeastern Center for Air Pollution and Epidemiology (SCAPE). Atmos. Meas. Tech. 8, 471–482.

Garçon, G., Dagher, Z., Zerimech, F., Ledoux, F., Courcot, D., Aboukais, A., Puskaric, E., Shirali, P., 2006. Dunkerque City air pollution particulate matter-induced cytotoxicity, oxidative stress and inflammation in human epithelial lung cells (L132) in culture. Toxicol. Vitro 20 (4), 519–528.

Guy, P.A., Gremaud, E., Richoz, J., Turesky, R.J., 2000. Quantitative analysis of mutagenic heterocyclic aromatic amines in cooked meat using liquid chromatography–atmospheric pressure chemical ionisation tandem mass spectrometry. J. Chromatogr. A 883 (1–2), 89–102.

Haan, D.O.D., Tolbert, M.A., Jimenez, J.L., 2009. Atmospheric condensed-phase reactions of glyoxal with methylamine. Geophys. Res. Lett. 36 (11). L11819.

Haan, D.O.D., Hawkins, L.N., Kononenko, J.A., Turley, J.J., Corrigan, A.L., Tolbert, M.A., Jimenez, J.L., 2011. Formation of nitrogen-containing oligomers by methylglyoxal and amines in simulated evaporating cloud droplets. Environ. Sci. Technol. 45 (3), 984.

Jin, L., Xie, J., Wong, C.K., Chan, S.K., Abbaszade, G.l., Schnelle-Kreis, J.r., Zimmermann, R., Li, J., Zhang, G., Fu, P., 2019. Contributions of city-specific fine particulate matter (PM2. 5) to differential in vitro oxidative stress and toxicity implications between Beijing and Guangzhou of China. Environ. Sci. Technol. 53 (5), 2881–2891.

Karlsson, H.L., Nilsson, L., Möller, L., 2005. Subway particles are more genotoxic than street particles and induce oxidative stress in cultured human lung cells. Chem. Res. Toxicol. 18 (1), 19–23.

Kiss, G., Varga, B., Galambos, I., Ganszky, I., 2002. Characterization of water-soluble organic matter isolated from atmospheric fine aerosol. J. Geophys. Res. Atmos. 107 (D21), 8339.

Krivacsy, Z., Kiss, G., Varga, B., Galambos, I., Sárvári, Z., Gelencser, A., Molnar, A., Fuzzi, S., Facchini, M., Zappoli, S., 2000. Study of humic-like substances in fog and interstitial aerosol by size-exclusion chromatography and capillary electrophoresis. Atmos. Environ. 34 (25), 4273–4281.

Kumagai, Y., Koide, S., Taguchi, K., Endo, A., Nakai, Y., Yoshikawa, T., Shimojo, N., 2002. Oxidation of proximal protein sulfhydryls by phenanthraquinone, a component of diesel exhaust particles. Chem. Res. Toxicol. 15 (4), 483–489.

Laskin, A., Smith, J.S., Laskin, J., 2009. Molecular characterization of nitrogen-containing organic compounds in biomass burning aerosols using high-resolution mass spectrometry. Environ. Sci. Technol. 43 (10), 3764–3771.

Leonard, N.J., 1960. Chapter 3 Senecio alkaloids. In: Manske, R.H.F. (Ed.), The Alkaloids: Chemistry and Physiology, vol. 6. Academic Press, pp. 35–121.

Li, N., Venkatesan, M.I., Miguel, A., Kaplan, R., Gujuluva, C., Alam, J., Nel, A., 2000. Induction of heme oxygenase-1 expression in macrophages by diesel exhaust particle chemicals and quinones via the antioxidant-responsive element. J. Immunol. 165 (6), 3393–3401.

Li, N., Xia, T., Nel, A.E., 2008. The role of oxidative stress in ambient particulate matter-induced lung diseases and its implications in the toxicity of engineered nanoparticles. Free Radic. Biol. Med. 44 (9), 1689–1699.

Li, Q., Wyatt, A., Kamens, R.M., 2009. Oxidant generation and toxicity enhancement of aged-diesel exhaust. Atmos. Environ. 43 (5), 1037–1042.

Li, C.; Fang, Z.; Czech, H.; Schneider, E.; Ruger, C. P.; Pardo, M.; Zimmermann, R.; Chen, J.; Laskin, A.; Rudich, Y. J. S. o. T. T. E., pH modifies the oxidative potential and peroxide content of biomass burning HULIS under dark aging. 2022, 834, 155365.

Lin, P., Yu, J.Z., 2011. Generation of reactive oxygen species mediated by humic-like substances in atmospheric aerosols. Environ. Sci. Techol. 45 (24), 10362–10368.

Lin, M., Yu, J.Z., 2019. Dithiothreitol (DTT) concentration effect and its implications on the applicability of DTT assay to evaluate the oxidative potential of atmospheric aerosol samples. Environ. Poll. 251, 938–944.

Lin, P., Rincon, A.G., Kalberer, M., Yu, J.Z., 2012. Elemental composition of HULIS in the Pearl River Delta Region, China: results inferred from positive and negative electrospray high resolution mass spectrometric data. Environ. Sci. Technol. 46 (14), 7454–7462.

Lin, P., Laskin, J., Nizkorodov, S.A., Laskin, A., 2015a. Revealing Brown carbon chromophores produced in reactions of methylglyoxal with ammonium sulfate. Environ. Sci. Technol. 49 (24), 14257.

Lin, P., Liu, J., Shilling, J.E., Kathmann, S.M., Laskin, J., Laskin, A., 2015b. Molecular characterization of brown carbon (BrC) chromophores in secondary organic aerosol generated from photo-oxidation of toluene. Phys. Chem. Chem. Phys. 17 (36), 23312–23325.

Lin, P., Fleming, L.T., Nizkorodov, S.A., Laskin, J., Laskin, A., 2018. Comprehensive molecular characterization of atmospheric Brown carbon by high resolution mass spectrometry with electrospray and atmospheric pressure photoionization. Anal. Chem. 90 (21), 12493–12502.

Ma, Y., Hays, M.D., 2008. Thermal extraction–two-dimensional gas chromatography–mass spectrometry with heart-cutting for nitrogen heterocyclics in biomass burning aerosols. J. Chromatogr. A 1200 (2), 228–234.

McLafferty, F., Tureček, F., 1993. Interpretation of Mass Spectra, fourth ed. University Science Books.

Oh, S.M., Kim, H.R., Park, Y.J., Lee, S.Y., Chung, K.H., 2011. Organic extracts of urban air pollution particulate matter (PM2. 5)-induced genotoxicity and oxidative stress in human lung bronchial epithelial cells (BEAS-2B cells). Mutat. Res., Genet. Toxicol. Environ. Mutagen. 723 (2), 142–151.

Pluskal, T., Castillo, S., Villar-Briones, A., Orešič, M., 2010. MZmine 2: modular framework for processing, visualizing, and analyzing mass spectrometry-based molecular profile data. BMC Bioinf. 11 (1), 395.

Pope 3rd, C., Bates, D.V., Raizenne, M.E., 1995a. Health effects of particulate air pollution: time for reassessment? Environ. Health Perspect. 103 (5), 472–480.

Pope, C.A., Thun, M.J., Namboodiri, M.M., Dockery, D.W., Evans, J.S., Speizer, F.E., Heath, C.W., 1995b. Particulate air pollution as a predictor of mortality in a prospective study of US adults. Am. J. Respir. Crit. Care Med. 151 (3), 669–674.

Saffari, A., Daher, N., Shafer, M.M., Schauer, J.J., Sioutas, C., 2014. Seasonal and spatial variation in dithiothreitol (DTT) activity of quasi-ultrafine particles in the Los Angeles Basin and its association with chemical species. J. Environ. Sci. Health, Part A 49 (4), 441–451.

Samy, S., Robinson, J., Rumsey, I.C., Walker, J.T., Hays, M.D., 2013. Speciation and trends of organic nitrogen in southeastern US fine particulate matter (PM2. 5). J. Geophys. Res. Atmos. 118 (4), 1996–2006.

Sedehi, N., Takano, H., Blasic, V.A., Sullivan, K.A., Haan, D.O.D., 2013. Temperature- and pH-dependent aqueous-phase kinetics of the reactions of glyoxal and methylglyoxal with atmospheric amines and ammonium sulfate. Atmos. Environ. 77 (Oct), 656–663.

See, S., Wang, Y., Balasubramanian, R., 2007. Contrasting reactive oxygen species and transition metal concentrations in combustion aerosols. Environ. Res. 103 (3), 317–324.

Shirmohammadi, F., Wang, D., Hasheminassab, S., Verma, V., Schauer, J.J., Shafer, M. M., Sioutas, C., 2017. Oxidative potential of on-road fine particulate matter (PM2. 5)

measured on major freeways of Los Angeles, CA, and a 10-year comparison with earlier roadside studies. Atmos. Environ. 148, 102–114.
Tai, A., Aburada, M., Ito, H., 2014. A simple efficient synthesis and biological evaluation of 3-O-ethylascorbic acid. Biosci. Biotechnol. Biochem. 78 (12), 1984–1987.
Tuet, W.Y., Chen, Y., Xu, L., Fok, S., Gao, D., Weber, R.J., Ng, N.L., 2017. Chemical oxidative potential of secondary organic aerosol (SOA) generated from the photooxidation of biogenic and anthropogenic volatile organic compounds. Atmos. Chem. Phys. 17 (2), 839–853.
Valavanidis, A., Vlachogianni, T., Fiotakis, K., Loridas, S., 2013. Pulmonary oxidative stress, inflammation and cancer: respirable particulate matter, fibrous dusts and ozone as major causes of lung carcinogenesis through reactive oxygen species mechanisms. Int. J. Environ. Res. Publ. Health 10 (9), 3886–3907.
Vandana, G., Saroj, A., Dhriti, K., Renu, B., 2014. Free radical scavenging activity and HPLC analysis of Araucaria cunninghamii Aiton ex D. Don leaf extract. J. Stress Physiol. Biochem. 10 (3), 176–185.
Verma, V., Rico-Martinez, R., Kotra, N., King, L., Liu, J., Snell, T.W., Weber, R.J., 2012. Contribution of water-soluble and insoluble components and their hydrophobic/hydrophilic subfractions to the reactive oxygen species-generating potential of fine ambient aerosols. Environ. Sci. Technol. 46 (20), 11384–11392.
Verma, V., Fang, T., Guo, H., King, L., Bates, J., Peltier, R., Edgerton, E., Russell, A., Weber, R., 2014. Reactive oxygen species associated with water-soluble PM 2.5 in the southeastern United States: spatiotemporal trends and source apportionment. Atmos. Chem. Phys. 14 (23), 12915–12930.
Verma, V., Fang, T., Xu, L., Peltier, R.E., Russell, A.G., Ng, N.L., Weber, R.J., 2015a. Organic aerosols associated with the generation of reactive oxygen species (ROS) by water-soluble PM2. 5. Environ. Sci. Technol. 49 (7), 4646–4656.
Verma, V., Wang, Y., El-Afifi, R., Fang, T., Rowland, J., Russell, A.G., Weber, R.J., 2015b. Fractionating ambient humic-like substances (HULIS) for their reactive oxygen species activity–Assessing the importance of quinones and atmospheric aging. Atmos. Environ. 120, 351–359.
Vidrio, E., Phuah, C.H., Dillner, A.M., Anastasio, C., 2009. Generation of hydroxyl radicals from ambient fine particles in a surrogate lung fluid solution. Environ. Sci. Technol. 43 (3), 922–927.
Wang, J., Lin, X., Lu, L., Wu, Y., Zhang, H., Lv, Q., Liu, W., Zhang, Y., Zhuang, S., 2018. Temporal variation of oxidative potential of water soluble components of ambient PM2.5 measured by dithiothreitol (DTT) assay. Sci. Total Environ. 649, 969–978.
Wei, J., Fang, T., Wong, C., Lakey, P.S., Nizkorodov, S.A., Shiraiwa, M., 2020. Superoxide formation from aqueous reactions of biogenic secondary organic aerosols. Environ. Sci. Technol. 55 (1), 260–270.
Xia, J.L., Fan, X., You, C.Y., Wei, X.Y., Zhao, Y.P., Cao, J.P., 2016. Sequential ultrasonic extraction of a Chinese coal and characterization of nitrogen-containing compounds in the extracts using high-performance liquid chromatography with mass spectrometry. J. Separ. Sci. 39 (13), 2491–2498.
Yiqiu, M., Yubo, C., Xinghua, Q., Gang, C., Yanhua, F., Junxia, W., Tong, Z., Jianzhen, Y., Di, H., 2018. Sources and oxidative potential of water-soluble humic-like substances (HULISWS) in fine particulate matter (PM2.5) in Beijing. Atmos. Chem. Phys. 18, 1–14.
Yu, H., Wei, J., Cheng, Y., Subedi, K., Verma, V., 2018. Synergistic and antagonistic interactions among the particulate matter components in generating reactive oxygen species based on the dithiothreitol assay. Environ. Sci. Technol. 52 (4), 2261–2270.
Zhou, P., Kong, Y., Cui, X., 2022. Inhalation Bioaccessibility of Polycyclic Aromatic Hydrocarbons in PM2. 5 under Various Lung Environments: Implications for Air Pollution Control during Coronavirus Disease-19 Outbreak. Environ. Sci. Technol 56 (7), 4272–4281.